



# Noise shielding using active acoustic metamaterials with electronically tunable acoustic impedance

Pavel MOKRÝ<sup>1</sup>; Kateřina STEIGER<sup>2</sup>; Jan VÁCLAVÍK<sup>1</sup>; Pavel PSOTA<sup>2</sup>; Roman DOLEČEK<sup>2</sup>; Pavel MÁRTON<sup>1</sup>; Miloš KODEJŠKA<sup>1</sup>; Martin ČERNÍK<sup>1</sup>

<sup>1</sup> Technical University of Liberec, Czech Republic

<sup>2</sup> Regional Center for Special Optics and Optoelectronic Systems TOPTEC, Czech Republic

## ABSTRACT

Noise pollution has become one of the most serious problems of our society. Considerable part of unpleasant noise is transmitted into the interior of buildings through large vibrating planar structures - windows with poor noise-isolation properties caused by their low flexural rigidity. In this Paper, we demonstrate and analyze a noise shielding using an active acoustic metamaterial (AAMM) with electronically tunable acoustic impedance. The AAMM consists of a curved glass plate with attached piezoelectric Macro-Fiber Composite (MFC) actuators shunted by negative capacitor (NC) circuits. Using this approach, it is possible to electronically control the effective elasticity of the MFC actuators and, therefore, the flexural rigidity of the composite structure of the AAMM. Key features that control the acoustic impedance of the AAMM have been analyzed on a simplified analytical model. Frequency dependence of the acoustic impedance and the acoustic transmission loss through the AAMM are measured and compared. Vibration modes of the AAMM are optically measured using Digital Holographic Interferometry (DHI).

Keywords: Active Acoustic Metamaterial, Noise Shielding, Electronic Control of Acoustic Impedance  
I-INCE Classification of Subjects Number(s): 33, 35.2.2

## 1. INTRODUCTION

Nowadays, increased noise levels in urban areas represent an everlasting environmental problem with severe deteriorating effect on human health. It is known that a great part of disturbing noise is generated by vibrating structures of large planar areas such as windows, flexible cover panels, glass facades, etc. A considerable path for noise penetrating the building interior is represented by glass windows. The low noise shielding efficiency of large planar structures is caused by low values of their flexural rigidity. This is the reason for our intense research focus on the noise shielding through glass plates, which constitutes the essential parts of windows.

Generally, passive noise control methods are not acceptably efficient in the case of large flexible panels, especially in frequency range below 1 kHz. Several methods for passive noise shielding through windows are available such as double glazed panels and laminated glass plates (1). These methods are efficient in reducing the noise transmission at frequencies higher than 1 kHz. On the other hand, noise shielding efficiency of double glazed windows deteriorates rapidly below their resonance frequency, where their noise isolation can be even worse than that of a single glass plate.

Similarly, several noise shielding systems based on the active noise control have been demonstrated, e.g. the feedforward and adaptive feedback controller of sound transmission through double-glazed windows by Jakob and Möser (2, 3). Another example of the active noise control approach to be mentioned here is the active structural acoustic control, which has been developed for the reduction of the structure-borne noise. One of the pioneering works demonstrating the active vibration control of large planar structures and the potential efficiency of piezoelectric actuators was presented by Fuller et al. (4). Thereafter, various methods of active structural acoustic control has been applied to passive double panel systems, in order to enhance the noise control performance, e.g. Carneal and Fuller (5) or Li and Cheng (6). Unfortunately, application of pure active methods to windows requires a good understanding of structural-acoustic interactions in the considered system. In addition, robust and complex control algorithms put high demands on the computational performance of digital electronics. As a result, in general, such requirements yield rather expensive and energy consuming

---

<sup>1</sup>pavel.mokry@tul.cz

systems.

In the presented Paper, an alternative approach to noise transmission suppression is presented. A reasonable noise shielding effect can be achieved using the semi-active control approach. It is known that, when the incident acoustic wave hits a glass plate, a part of the wave is reflected, which makes the glass plate vibrate. This vibration represents a sound source for the transmitted acoustic wave. It can be easily shown that the greater the amplitude of the glass plate vibration in the normal direction, the greater the amount of acoustic energy is transmitted through the glass plate. It is clear that the vibration amplitude depends on the specific acoustic impedance of the glass plate. Usually it holds that the higher the mass density of the glass plate, the higher the value of its specific acoustic impedance is. Unfortunately, a weight increase of a light-weight structure is frequently unwanted in many practical applications. Therefore, our interest is focused on finding ways to increase the value of specific acoustic impedance of the glass plate without increasing the weight of the structure. Our approach is based on implementation of the composite glass shell with active piezoelectric actuators connected to the electronic shunt circuits. In fact, the system fabricated in this way is often called an Active Acoustic Metamaterial (AAMM), see e.g. (7, 8). This method profitably balances the advantages of both passive and active approaches: a high efficiency, a simple technical implementation, a minimal weight and size, a low cost, and small external power supply.

In our recent work, a numerical simulation of the acoustic transmission loss through the considered AAMM system has been performed using Finite Element Method (FEM). Results of these simulations indicated a possibility to increase the acoustic transmission loss by more than 20 dB in the frequency range up to 1 kHz (9). Subsequent measurements of the acoustic transmission loss demonstrated that it is possible to achieve an increase in the value of acoustic transmission loss through the glass window by about 10 dB. Unfortunately, these values have been gained only in a narrow frequency range. In this work, the design of the improved noise shielding system has been carried out.

## 2. NOISE SHIELDING USING ACTIVE ACOUSTIC METAMATERIALS

In this section, a brief explanation of the noise shielding principles using AAMM is presented.

### 2.1 Noise shielding principles

Due to their physical nature, noise and vibrations are accompanied with the flow of mechanical or acoustic energy. Propagation of acoustic energy in a material and the reflection of acoustic waves at interfaces of two different materials are controlled by a physical property called acoustic impedance  $Z$  (in  $\text{Pa s m}^{-3}$ ). It is a frequency-dependent parameter defined as an acoustic sound pressure  $p$  divided by particle velocity  $v$  and a surface area  $S$ , through which an acoustic wave propagates:

$$Z = p/(vS). \quad (1)$$

When dealing with planar structures, it is often convenient to express the acoustic impedance per unit area of the structure by introducing a physical property called specific acoustic impedance (in  $\text{Pa s m}^{-1}$ ). If a sound wave propagates through a medium, its wave motion is characterized by a physical property called characteristic acoustic impedance  $z_0$  (in  $\text{Pa s m}^{-1}$ ):

$$z_0 = \sqrt{\rho B}. \quad (2)$$

where symbols  $\rho$  and  $B$  stand for the mass density and the bulk modulus of the medium, respectively.

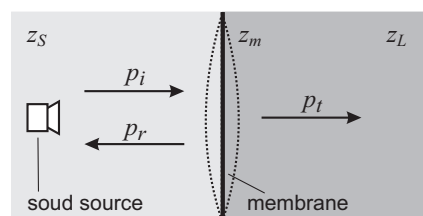


Figure 1 – The sound reflection and transmission at the interface of the two media with different characteristic acoustic impedances  $z_S$  and  $z_L$ , and separated by a membrane with specific acoustic impedance  $z_m$ .

The role of acoustic impedance in noise and vibration suppression devices can be easily demonstrated on a simple example shown in Fig. 1. Consider an interface of two acoustic media with different characteristic acoustic impedances  $z_S$  and  $z_L$ . The interface is represented by a membrane with a specific acoustic impedance  $z_m$ . Consider a sound source on the left hand side of the membrane that produces an (incident) sound wave of

the acoustic pressure amplitude  $p_i$ . At the interface, a part of the wave is reflected and a part is transmitted. The acoustic pressure amplitudes of reflected and transmitted waves are denoted by symbols  $p_r$  and  $p_t$ . In this system, it is convenient to define reflection,  $C_r = p_r/p_i$ , and transmission coefficients,  $C_t = p_t/p_i$ . In order to calculate values of  $C_r$  and  $C_t$ , one should solve the equation of motion for the membrane  $p_i + p_r - p_t = z_m v$  and equations for the continuity of particle velocity at the interface  $v = p_t/z_L = (p_i - p_r)/z_S$ . As a result, the reflection and transmission coefficients can be expressed in terms of the acoustic impedances in the system:

$$C_r = \frac{z_L + z_m - z_S}{z_L + z_m + z_S}, \quad \text{and} \quad C_t = \frac{2z_L}{z_L + z_m + z_S}. \quad (3)$$

It is convenient to express the amount of transferred acoustic potential energy in the decibel scale by introducing the physical quantity called acoustic transmission loss  $TL = 20 \log_{10} |1/C_t|$ . When the characteristic acoustic impedance at the both sides of the membrane is the same, i.e.  $z_S = z_L = z_a$  the acoustic transmission loss has the well known form:

$$TL = 20 \log_{10} \left| 1 + \frac{z_m}{2z_a} \right|, \quad (4)$$

where  $z_a = \rho_0 c$  is the characteristic acoustic impedance of air, where  $\rho_0$  is the air density and  $c$  is the sound velocity in the air.

Now consider that one can control the value of the specific acoustic impedance of the membrane  $z_m$ . By looking at formulas given by Eq. (3), one can identify two situations of practical interest: (i) When  $z_m = z_S - z_L$ , the value of reflection coefficient reaches zero and no sound is reflected from the interface. Such a situation can be described as a perfectly absorbing surface. (ii) When  $z_m$  goes to infinity, the value of transmission coefficient goes to zero and all acoustic energy is reflected back to the source. Such a system can be interpreted as a perfect sound shield.

## 2.2 Active acoustic metamaterial

It is clear that a construction of the perfect sound shield, which efficiently controls the noise transmission, usually requires values of acoustic impedance that are not observed in nature. Such systems are often called tunable or active acoustic metamaterial (AAMM), see e.g. Refs. (7, 8). The key objective of the this Paper is to study methods for the precise active control of acoustic impedance of large planar structures. We will show that an efficient approach to control the acoustic impedance of the vibrating structure is to use piezoelectric transducers which are connected to passive or active electronic shunt circuits.

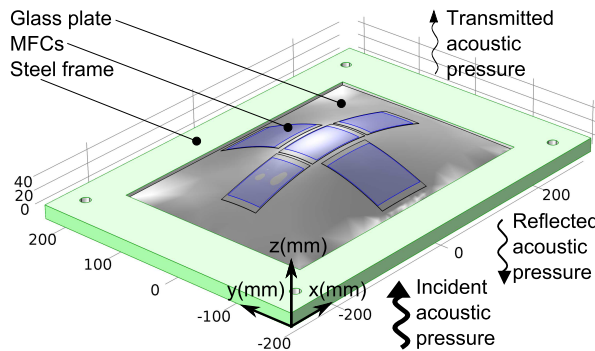


Figure 2 – 3D model of the considered active acoustic metamaterial, which consists of the curved glass plate fixed in a rigid steel frame at its edges and with macro fiber composite actuators (MFCs) attached. An incident sound wave of the acoustic pressure strikes the glass plate. It makes the glass plate vibrate and a part of the sound wave is reflected and a part is transmitted.

We consider an AAMM, which consists of a curved glass plate of thickness  $h_g$  and inverse radius of curvature  $\xi$ . The curved glass plate is fixed at its edges in a rigid steel frame of inner dimensions  $a$  and  $b$ . On the top surface of the glass plate, piezoelectric Macro Fiber Composite (MFC) actuators of thickness  $h_{MFC}$  are attached as it is shown in Fig. 2. The use of flexible piezoelectric fibers reinforced MFC composite eliminates potential problems of fragile vibrating structures such as glass plates. More details can be found in Ref. (10). The successful implementation of the considered approach essentially depends on the correct placement of MFC actuators on the AAMM surface due to the complicated distribution of nodes and antinodes. For that reason, the detailed measurement of vibration mode profiles of the AAMM has been carried out using Digital Holographic Interferometry (DHI) measurements (11). The presented configuration of MFCs is selected in

order to allow the suppression of majority of low-frequency vibrational modes as it was analyzed and discussed in Ref. (12).

According to the analytical model of the generally curved glass shell of rectangular shape and the FEM model of the planar and curved glass plate computed by Nováková et al. (9), the specific acoustic impedance of the curved rectangular glass shell can be approximated in the frequency range near the lowest resonant frequency of the curved rectangular glass plate by the formula:

$$z_m(\omega) \approx \frac{\pi^2 (G \zeta + 2Yh\xi^2 - (1-\nu)\rho h\omega^2)}{8i\omega a^2 b^2 (1-\nu)}, \quad (5)$$

where

$$\zeta = \pi^4 (1-\nu)^2 (1+\nu) [1/b^2 + 1/a^2]^2, \quad (6)$$

$$Y = \frac{Y_g h_g + Y_{\text{MFC}} h_{\text{MFC}}}{h_g + h_{\text{MFC}}}, \quad (7)$$

$$G = \frac{Y_g^2 h_g^4 + Y_{\text{MFC}}^2 h_{\text{MFC}}^4 + 2Y_g Y_{\text{MFC}} h_g h_{\text{MFC}} (2h_g^2 + 3h_g h_{\text{MFC}} + 2h_{\text{MFC}}^2)}{12(1-\nu^2)(Y_g h_g + Y_{\text{MFC}} h_{\text{MFC}})}, \quad (8)$$

and symbols  $Y_g$ ,  $\nu$ , and  $\rho$  stand for the Young's modulus, Poisson ratio, and mass density of the glass plate. Symbol  $Y_{\text{MFC}}$  stands for the Young's modulus of the piezoelectric MFC actuator. Symbol  $\omega$  is the angular frequency of the incident sound wave, and  $i = \sqrt{-1}$ .

It is clearly seen from Eqs. (5)-(8) that the higher the value of macroscopic Young's modulus of the MFC actuator, the higher the value of its specific acoustic impedance  $z_m$  of the whole AAMM is. At some given frequency  $\omega$  in the frequency range near the lowest resonant frequency of the curved rectangular glass plate, the formula given by Eq. (5) actually represents a one-to-one mapping between the complex values of  $Y_{\text{MFC}}$  and  $z_m$ . It is convenient to denote this mapping by a symbol  $g_\omega$ , i.e.  $z_m = g_\omega(Y_{\text{MFC}})$ .

In order to control the macroscopic elastic properties of piezoelectric actuator, we adopt the method by Date et al. (13).

### 2.3 Active elasticity control

Date et al. (13) have developed a method to control the elastic properties of piezoelectric actuator by connecting them to active shunt circuits. It is a straightforward task to show that the macroscopic value of the Young's modulus  $Y_{\text{MFC}}$  of the piezoelectric actuator of capacitance  $C_S$ , which is shunted by an external shunt circuit with a capacitance  $C$ , is equal to:

$$Y_{\text{MFC}} = Y_S \left( 1 + \frac{k^2}{1 - k^2 + C/C_S} \right), \quad (9)$$

where  $Y_S$  is the Young's modulus of piezoelectric MFC actuator material with short-circuited electrodes,  $k$  is the electromechanical coupling factor. Formula given by Eq. (9) actually represents one-to-one mapping between the complex planes of values of external capacitance  $C$  and Young's modulus  $Y_{\text{MFC}}$ , see Ref. (14). It will be convenient to denote this mapping by a symbol  $f$ , i.e.  $Y_{\text{MFC}} = f(C)$ .

It follows from Eq. (9) that for positive values of the shunt circuit capacitance  $C$ , the effective value of Young's modulus can be changed by an approximately 50% of the ordinary value. On the other hand, when the shunt circuit capacitance  $C$  is negative, it is possible to identify three regimes of active elasticity control: (i) When  $C/C_S < -1$ , the effective Young's modulus is smaller than the ordinary value,  $0 < Y_{\text{MFC}} \ll Y_S$ , and the actuator becomes softer. (ii) When  $C/C_S > -1 + k^2$ , the effective Young's modulus is greater than the ordinary value  $Y_{\text{MFC}} \gg Y_S$  and the actuator becomes harder. (iii) When  $-1 < C/C_S < -1 + k^2$ , the effective value of Young's modulus is negative, i.e.  $Y_{\text{MFC}} < 0$ .

In order to achieve the arbitrary value of the Young's modulus of a piezoelectric material, Date et al. (13) suggested to connect a circuit with a negative capacitance (NC). Therefore, it is possible to establish a direct coupling between the values of the specific acoustic impedance  $z_m$  of the AAMM and the value of the connected shunt circuit capacitance  $C$ :

$$z_m = g_\omega(f(C)). \quad (10)$$

Since under the conditions specified above, the both functions  $f$  and  $g_\omega$  are one-to-one mappings between two complex planes, there exist inverse functions  $f^{-1}$  and  $g_\omega^{-1}$ . Then, it possible to find a value of the shunt capacitance  $C$ , which yield the required value of the specific acoustic impedance  $z_m$ :

$$C = f^{-1}(g_\omega^{-1}(z_m)). \quad (11)$$

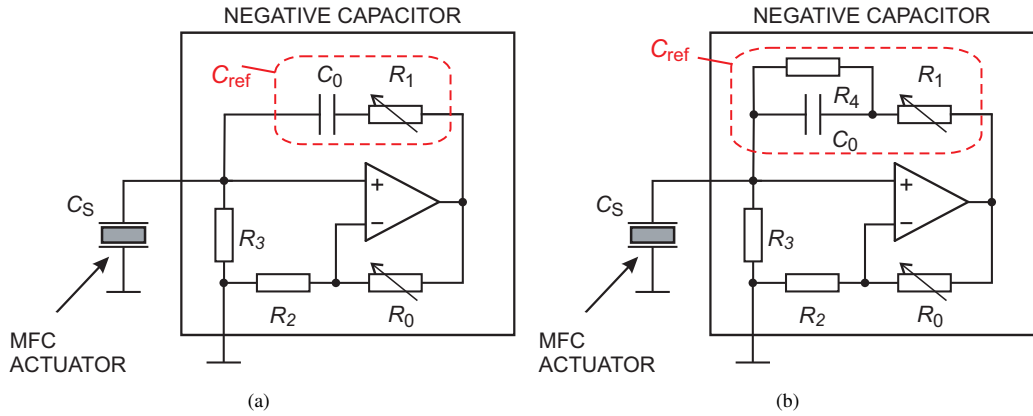


Figure 3 – Electrical schemes of the negative capacitance circuits connected to the Macro Fiber Composite (MFC) actuators in our experimental work for narrow (a) and broad (b) frequency range noise suppression.

Since the perfect noise shield requires large values of  $z_m$  of the AAMM, i.e.  $|z_m| \rightarrow \infty$ , it is immediately seen from Eqs. (5) and (9) that required values of the external capacitance should converge to  $C \rightarrow -(1 - k^2)C_S$ . For this purpose, the active circuits shown in Fig. 3 have been adopted as external shunt circuit to the MFC actuators. The adopted circuits have a negative effective capacitance:

$$C_{NC} = -\frac{R_0}{R_2}C_{ref} - \frac{i}{\omega R_3}, \quad (12)$$

where reference capacitance  $C_{ref}$  was implemented in two versions of the  $RC$ -network for narrow band (NB) and broad band (BB) noise shielding:

$$C_{ref}^{(NB)} = \frac{C_0}{1 + j\omega C_0 R_1}, \quad (13)$$

$$C_{ref}^{(BB)} = \frac{\omega C_0 R_4 - i}{\omega (R_1 + R_4 + i\omega C_0 R_1 R_4)}. \quad (14)$$

It is seen from Eqs. (12)-(14) that at given frequency  $\omega$ , it is possible to adjust resistances  $R_0$  and  $R_1$  in such a way that the real and imaginary parts of the shunt circuit capacitance satisfy conditions given by Eq. (11).

The experimental verification of the above described approach is presented in the next section.

### 3. EXPERIMENTAL METHODS

In this section, a brief description of experimental methods will be given.

#### 3.1 Fabrication of the active acoustic metamaterial

It is known that the efficiency of the noise shielding can be enhanced by making the AAMM surface curved (15). The curved shape of the glass plate was produced as follows: First, the glass shaping mold with the profile  $z_{max} \sin(\pi x/a) \sin(\pi y/b)$ , where  $a = 0.42$  m,  $b = 0.3$  m, and  $z_{max} = 5$  mm has been cut into an iron block using Computer Numerical Control cutting machine. The flat glass of the thickness 4 mm and dimensions  $0.445$  m  $\times$   $0.318$  m was put on top of the iron mold and thermally treated in the oven to achieve its lying down to the mold and forming a curved glass plate of the above specified profile.

The MFC actuators were attached using an epoxy glue on the top surface of the curved glass shell. Negative capacitance circuit was connected to shunt all MFC actuators. Finally, the curved glass plate with attached MFC actuators was clamped in an iron frame of the inner dimensions  $0.42$  m  $\times$   $0.3$  m.

#### 3.2 Measurement of the specific acoustic impedance

Figure 4(a) shows the experimental setup for the approximative measurements of the specific acoustic impedance. The fabricated AAMM forms a lid of the soundproof box with a loudspeaker UNI-PEX P-500 that produces the source of the incident sound wave. The microphone IN, inside the box, and the microphone OUT, outside the soundproof box, measure the acoustic pressures difference  $\Delta p$ . The microphones are located approximately 1 cm above and below the middle point of the glass plate. A laser Doppler vibrometer measures the amplitude of the vibration velocity  $V$  of the selected (usually the middle) point of the glass plate. The

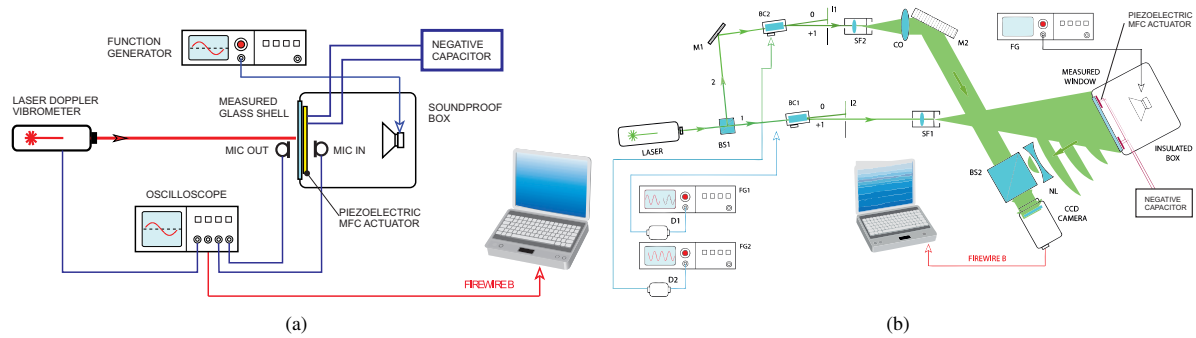


Figure 4 – Scheme of the acoustic TL approximative measurement. The glass plate forms a lid of the soundproof acoustic box with a loudspeaker as a source of the noise. MIC IN and MIC OUT measure the acoustic pressures difference at the opposite sides of the plate. Laser Doppler vibrometer measures the vibration velocity amplitude of the plate middle point. DAQ module collects and transfers measured data into the computer where the acoustic TL is computed. (a). Scheme of the digital holographic experimental setup: BC- Bragg Cells, BS - Beam Splitter, I - Iris Aperture, SF - Spatial Filter, M - Mirror, FG - Function Generator, D - Driver, CO - Collimating Lens. (b)

specific acoustic impedance  $z_m$  is approximated by the ratio:

$$z_m \approx \Delta p / V. \quad (15)$$

The values of TL are computed with the use of Eq. (4). Using such a simple measurement setup, only an approximative value of the TL can be obtained because of the limited dimensions of the box. It is, however, acceptable for the demonstration of the noise suppression efficiency.

### 3.3 Digital holography experimental setup

Figure 4(b) shows the digital holographic setup, which is based on the Mach-Zehnder type of holographic interferometer. The laser beam has a wavelength of 532 nm and power of 100 mW. After the mechanical shutter, the beam is split by the polarizing beam splitter, equipped with half wavelength retardation plates in two beams. Half wavelength retardation plates help set the intensities in both beams as well as the polarization of each beam. The first beam acts as a reference wave and could be further attenuated if necessary by a set of gray filters placed in filter wheels. Each beam is frequency shifted by an acousto-optic frequency modulator - Bragg cell, with a fundamental frequency of 40 MHz. The beams are spatially filtered and the reference one is collimated. The object beam illuminates the measured window and the light scattered from its surface interfere with the reference wave. The negative lens reduces the imaging angle and therefore the measured window having size  $425 \times 300$  mm can be measured. The camera has a resolution of  $2048 \times 2048$  pixels, each pixel having the size  $1.75 \times 1.75 \mu\text{m}$ . The camera is connected to the computer via a USB interface enabling a frame rate of 6.5 FPS.

The vibration profile of the AAMM at given frequency was computed using methods presented in Ref. (11).

## 4. RESULTS

At first, the acoustic transmission loss through the curved glass shell was measured in the frequency range from 150 Hz to 2 kHz. Then, two frequencies of 258 Hz and 1.46 kHz were identified with minimum values of the acoustic transmission loss. These frequencies corresponds to two dominant vibration modes of the AAMM.

Figure 5(a) shows the frequency dependences of the acoustic TL through the AAMM with short-circuited MFC actuators. After that, the NC circuit was adjusted according Eq. (11) and connected to the MFC actuators. The frequency dependence of the acoustic transmission loss was measured again. Effects of the shunt circuits connected to the MFC actuators on the change in the acoustic transmission loss is shown in Fig. 5(b).

Profiles of the vibration modes of the AAMM were measured using DHI. Figure 6 shows the profile of the vibration mode at the frequency 258 Hz, when the connected NC circuit was off 6(a) and on 6(b). Figure 7 shows the profile of the vibration mode at the frequency 1460 Hz, when the connected NC circuit was off 7(a) and on 7(b).

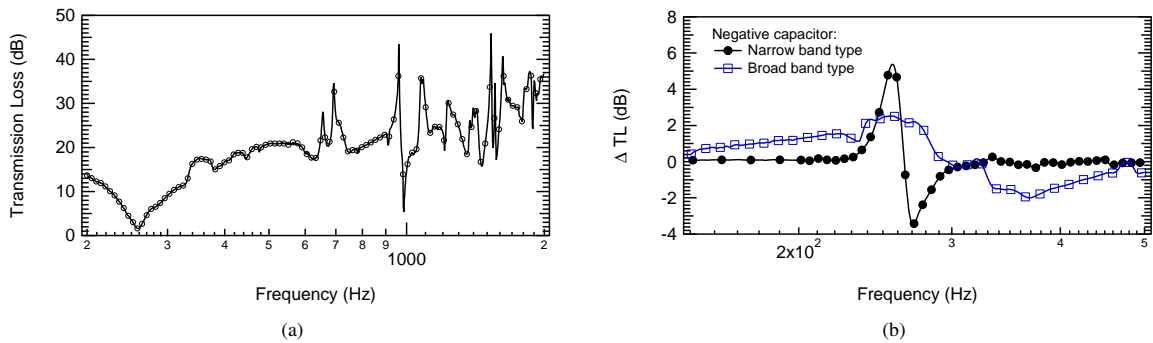


Figure 5 – Frequency dependences of the acoustic TL through the curved glass plate with attached MFC actuators with short-circuited electrodes (a). Increase in the acoustic transmission loss achieved due to the action of the active shunt circuit in the AAMM for narrow frequency band noise isolation (filled circles) and broad frequency band noise isolation (empty squares) (b).

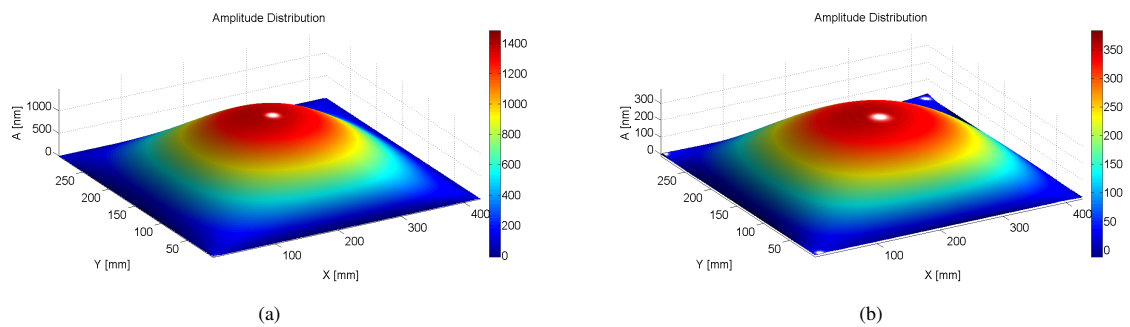


Figure 6 – Profile of the vibration mode of the curved glass shell at the frequency 258 Hz, when the connected NC circuit was off (a) and on (b).

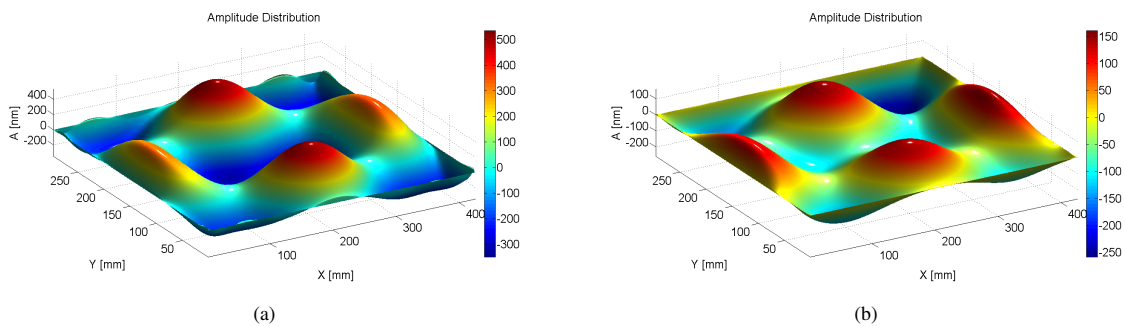


Figure 7 – Profile of the vibration mode of the curved glass shell at the frequency 1460 Hz, when the connected NC circuit was off (a) and on (b).

## 5. CONCLUSIONS

The noise shielding system, which is based on the Active Acoustic Metamaterial (AAMM), has been fabricated and analyzed experimentally. The AAMM consists of the curved glass plate with attached piezoelectric Macro Fiber Composite (MFC) actuators connected to the negative capacitor circuit. The approximative measurements of the acoustic transmission loss as a function of frequency have been carried out. Digital Holographic Interferometric (DHI) measurements of the AAMM vibration profile were carried out for frequencies 258 Hz and 1.46 kHz.

Two negative capacitance (NC) circuits were constructed and connected to the MFC actuators of the AAMM. The circuits were adjusted to suppress the vibration amplitude of the AAMM vibration mode at 258 Hz. Using this approach, the increase in the acoustic transmission loss has been achieved. The first circuit enhanced the noise shielding efficiency by 6 dB in the narrow frequency range. The second circuit enhanced the noise shielding efficiency by 3 dB but in much broader frequency range.

We believe that using further improvements in the design NC circuits, it is possible to achieve much more efficient suppression of the noise transmission in the broad range of frequencies.

## ACKNOWLEDGEMENTS

This work was supported by Czech Science Foundation Project No.: GACR 13-10365S, co-financed from Ministry of Education, Youth and Sports of the Czech Republic in the Project No. NPU LO1206.

## REFERENCES

1. Spagnolo R. *Manuale di acustica applicata*. UTET Università; 2001.
2. Jakob A, Moser M. Active control of double-glazed windows. Part II: Feedback control. *Applied Acoustics*. 2003 Feb;64(2):183–196.
3. Jakob A, Moser M. Active control of double-glazed windows - Part I: Feedforward control. *Applied Acoustics*. 2003 Feb;64(2):163–182.
4. Fuller CC, Elliott S, Nelson PA. *Active Control of Vibration*. Academic Press; 1996.
5. Carneal JP, Fuller CR. An analytical and experimental investigation of active structural acoustic control of noise transmission through double panel systems. *Journal Of Sound And Vibration*. 2004 May;272(3-5):749–771.
6. Li YY, Cheng L. Active noise control of a mechanically linked double panel system coupled with an acoustic enclosure. *Journal of Sound and Vibration, Short Communication*. 2006;297:1068–1074.
7. Akl W, Baz A. Multi-cell Active Acoustic Metamaterial with Programmable Bulk Modulus. *Journal of Intelligent Material Systems and Structures*. 2010 Mar;21(5):541–556. Available from: <http://jim.sagepub.com/cgi/doi/10.1177/1045389X09359434>.
8. Popa BI, Zigoneanu L, Cummer SA. Tunable active acoustic metamaterials. *Physical Review B*. 2013 Jul;88(2). Available from: <http://link.aps.org/doi/10.1103/PhysRevB.88.024303>.
9. Novakova K, Mokry P, Vaclavík J. Application of piezoelectric macro-fiber-composite actuators to the suppression of noise transmission through curved glass plates. *IEEE Transactions on Ultrasonics, Ferroelectrics and Frequency Control*. 2012 Sep;59(9):2004–2014. Available from: <http://ieeexplore.ieee.org/lpdocs/epic03/wrapper.htm?arnumber=6306022>.
10. Wilkie WK, Bryant RG, High JW, Fox RL, Hellbaum RF, Jalink A, et al. Low-cost piezocomposite actuator for structural control applications. In: Jacobs JH, editor. *Society of Photo-Optical Instrumentation Engineers (SPIE) Conference Series*. vol. 3991; 2000. p. 323–334.
11. Psota P, Ledl V, Dolecek R, Mokry P, Psota P, Dolecek R, et al. Measurement of vibration mode structure for adaptive vibration suppression system by digital holography. *IEEE*; 2013. p. 214–217. Available from: <http://ieeexplore.ieee.org/lpdocs/epic03/wrapper.htm?arnumber=6748749>.
12. Novakova K, Psota P, Dolecek R, Ledl V, Mokry P, Vaclavik J, et al. Planar acoustic metamaterials with the active control of acoustic impedance using a piezoelectric composite actuator. *IEEE*; 2013. p. 317–320. Available from: <http://ieeexplore.ieee.org/lpdocs/epic03/wrapper.htm?arnumber=6748720>.

13. Date M, Kutani M, Sakai S. Electrically controlled elasticity utilizing piezoelectric coupling. *Journal of Applied Physics*. 2000;87(2):863–868. NIC.
14. Mokřý P, Fukada E, Yamamoto K. Sound absorbing system as an application of the active elasticity control technique. *Journal of Applied Physics*. 2003;94(11):7356–7362. Available from: <http://link.aip.org/link/JAPIAU/v94/i11/p7356/s1&Agg=doi>.
15. Mokřý P, Fukada E, Yamamoto K. Noise shielding system utilizing a thin piezoelectric membrane and elasticity control. *Journal of Applied Physics*. 2003;94(1):789–796. Available from: <http://link.aip.org/link/JAPIAU/v94/i1/p789/s1&Agg=doi>.